Computational Materials Science 104 (2015) 205–211

Contents lists available at ScienceDirect

Computational Materials Science

journal homepage: www.elsevier.com/locate/commatsci

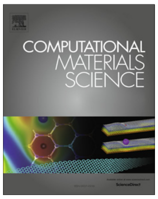

Ab-initio calculations for electronic structure and momentum densities of samarium sesquioxide

Sonu Sharma [a], N.L. Heda [b], K.K. Suthar [a], Samir Bhatt [a], Khushboo Sharma [a], B.L. Ahuja [a,*]

[a] Department of Physics, M.L. Sukhadia University, Udaipur 313001, Rajasthan, India
[b] Department of Pure & Applied Physics, University of Kota, Kota 324007, Rajasthan, India

ARTICLE INFO

Article history:
Received 29 January 2015
Received in revised form 31 March 2015
Accepted 2 April 2015
Available online 25 April 2015

Keywords:
Compton scattering
Electronic structure
Density functional theory

ABSTRACT

We report energy bands, partial and total density of states (DOS), Mulliken's population (MP) analysis and Compton profiles (CPs) of monoclinic and cubic Sm_2O_3 using linear combination of atomic orbitals scheme within local density and generalized gradient approximations (LDA and GGA). To compare the first ever theoretical momentum densities, we have measured for the first time the CP of cubic Sm_2O_3 using 20 Ci ^{137}Cs Compton spectrometer at an intermediate resolution of 0.34 a.u. The GGA calculations with Wu–Cohen exchange and Perdew–Burke–Ernzerhof correlation functionals give a better agreement with the experimental CP than different combinations of exchange and correlation potentials within density functional theory. The energy bands along with total DOS show a wide band gap behavior in both the phases. Further in case of monoclinic phase the MP data show unequal transfer of electrons from Sm to O sites, which are in contrast to cubic phase. Such a trend of MP data is also interpreted in terms of projected DOS of Sm_2O_3.

1. Introduction

The rare earth oxide Sm_2O_3 is a technologically important compound due to its various magnetic and electronic properties, energy and environmental related applications and its use in nuclear technology, optoelectronics, etc. [1–3]. Sm_2O_3 exists in two stable phases, namely monoclinic (B-type) and cubic (C-type) [1]. It exhibits C-phase at normal temperature and undergoes a phase transition from C-type to B-type at temperature above 800 °C. Among earlier studies, Raman scattering, absorption and photoluminescence measurements were performed by Martel et al. [1] for B- and C-type phases. B-type structure of Sm_2O_3 was also refined by Kennedy and Avdeev [3] using powder neutron diffraction data. White [4] has reported the diffuse-reflectance spectra for C-Sm_2O_3 and the value of the band gap was found to be 5.10 eV. A schematic energy band diagram for the genesis charge carries in B-Sm_2O_3 was reported by Lal and Gaur [5]. These authors have reported the experimental value of band gap as 2.12 eV. Atou et al. [6] have studied the pressure behavior at room temperature in B-Sm_2O_3 using X-ray diffraction method. Using photo-absorption measurements, periodicity in band gap variation was discussed by Prokofiev et al. [7]. The authors have reported the value of band gap as 5.0 eV for C-Sm_2O_3. Petit et al. [8] have applied the self-interaction-corrected local-spin-density approximation to describe the electronic structure of Sm_2O_3. On the basis of linear refractive index, Zhao et al. [9] have discussed energy gap and average electronic oxide polarizability of Sm_2O_3. Guo et al. [10] have reported density functional theory (DFT) calculations to obtain the phase transformation among hexagonal, B- and C-type phases and compared their results with the experimental data. Rahm and Skorodumova [11] have reported phase stability under pressure using DFT within local density approximation (LDA) and generalized gradient approximation (GGA). Also, a systematic investigation using many-body perturbation theory in the GW approach for the electronic properties were discussed by Jiang et al. [12]. Recently, Gillen et al. [13] have reported electronic structures of rare earth oxides including Sm_2O_3 using hybrid density functionals namely HSE03, HSE06 and screened exchange within DFT.

It is well established that measurement of double differential cross-section is a paramount mode for probing the ground state electron momentum densities (EMDs), $n(\vec{p})$ [14,15]. The study of EMDs through the Compton spectroscopy depends on the fulfillment of impulse approximation (IA), which allows the target electrons to be treated as free electrons. Within IA, the projection of EMD along z-axis (commonly accepted as the direction of scattering vector) is known as Compton profile (CP). Mathematically, $J(p_z)$ is written as

---

* Corresponding author. Tel.: +91 941 4317048; fax: +91 294 2411950.
E-mail address: blahuja@yahoo.com (B.L. Ahuja).

http://dx.doi.org/10.1016/j.commatsci.2015.04.001
0927-0256/

$$J(p_z) = \iint n(\vec{p})dp_x dp_y. \tag{1}$$

For the computation of EMD, $n(\vec{p})$, one can use the Fourier transformation of real space wave function [14,15].

To the best of our knowledge, electron momentum densities of both the B- and C-type Sm_2O_3 are still unexplored. In this paper, we report theoretical directional and isotropic CPs using DFT within LDA, GGA and second order GGA (SOGGA) within linear combination of atomic orbitals (LCAO) scheme. Further, we have also computed the energy bands, partial and total density of states (DOS), charge reorganization using Mulliken's population (MP) analysis, band gap, etc. for both B- and C-type Sm_2O_3. To validate the electronic structure calculations, we have also measured CP of C-type Sm_2O_3 using 661.65 keV photons.

2. Methodologies

2.1. Theory

We have employed the LCAO scheme [16] within DFT (LDA, GGA and SOGGA) to compute the electronic properties of B- and C-type Sm_2O_3. Within DFT scheme, the Hamiltonian operator (one particle) can be deduced from ground state electron density. In case of DFT-LDA, the exchange–correlation density functional energy (E_{XC}) is related to uniform charge density $n(r)$ as

$$E_{XC}^{LDA}[n(\mathbf{r})] = \int n(\mathbf{r}) \int \varepsilon_{XC}[n(\mathbf{r})]d\mathbf{r}. \tag{2}$$

where ε_{XC} is the exchange–correlation energy per particle.

In case of GGA, the ε_{XC} depends not only on the density but also on the gradient of the density $\nabla n(r)$ and defined as,

$$E_{XC}^{GGA}[n] = \int n(\mathbf{r})\varepsilon_{xc}^{GGA}[n(\mathbf{r}), \nabla n(\mathbf{r})]d\mathbf{r} \tag{3}$$

$$= \int \varepsilon_{xc}^{LDA}[r_s(\mathbf{r})]F_{XC}[r_s(\mathbf{r}), s(\mathbf{r})]d\mathbf{r} \tag{4}$$

In Eq. (3), ε_{xc}^{LDA} with uniform electron density n is given by,

$$\varepsilon_{xc}^{LDA} = -(3/4)(3/\pi)^{1/3}n^{4/3}, \tag{5}$$

and the multiplication factor $F_{xc}(r_s, s)$ is defined as,

$$F_{XC}(r_s, s) = F_X(s) + F_C(r_s, s), \tag{6}$$

where r_s and s are the Wigner–Seitz radius and reduced density gradient, respectively.

Mathematically, multiplication factor for exchange $F_x(s)$ is given as [18,20]

$$F_X^{WC}(s) = 1 + \kappa - (\kappa/(1 + ((0.123s^2 + (\mu - 0.123)s^2\exp(-s^2) + \ln(1 + cs^4))/\kappa))), \quad \text{for WC-GGA} \tag{7}$$

$$F_X^{SOGGA}(s) = 1 + \kappa + \frac{1}{2}\left(\frac{\kappa^2}{\kappa + \mu s^2}\right) - \frac{\kappa}{2}\left(e^{-(\mu/\kappa)s^2}\right), \quad \text{for SOGGA} \tag{8}$$

where μ and κ are the constants [18,20] and c is set to recover the fourth order parameters in F_x.

The combination of various exchange and correlation energies used in the present DFT calculations are as follows:

(i) In DFT-LDAPZ: The exchange energies of Dirac–Slater [16] and correlation energies of Perdew and Zunger [17].
(ii) In DFT-WCGGA: The exchange and correlation energies prescribed by Wu and Cohen [18] and Perdew–Becke–Ernzerhof [19], respectively.
(iii) DFT-SOGGA: The exchange energies of second order GGA [20] and correlation energies suggested by Perdew–Becke–Ernzerhof [19].

We have used the pseudopotential basis sets for Sm [21] and all-electron Gaussian basis sets for oxygen (O) [22]. The basis sets for Sm and O atoms were energy optimized using BILLY software [16]. The lattice parameters (a = 14.184 Å, b = 3.627 Å, c = 8.858 Å

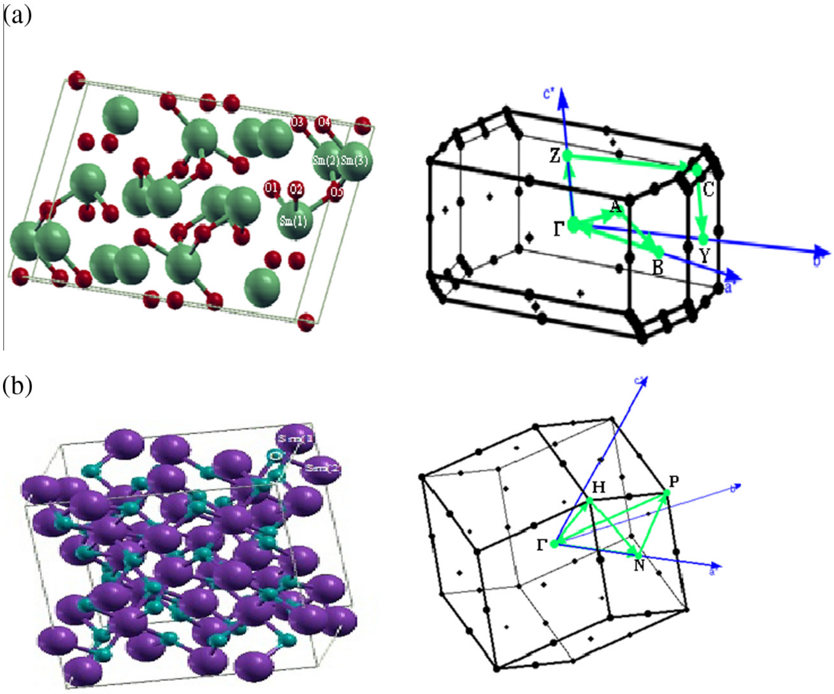

Fig. 1. Structural sketch (left hand side) and labeled Brillouin zone (right hand side) for (a) B-type (monoclinic) and (b) C-type (cubic) Sm_2O_3.